

Detection of serum uric acid using the optical polymeric enzyme biochip system

Su-Hua Huang^a, Yu-Chuan Shih^b, Chung-Yu Wu^b, Chiun-Jye Yuan^a,
Yuh-Shyong Yang^a, Yaw-Kuen Li^c, Tung-Kung Wu^{a,*}

^a Department of Biological Science and Technology, National Chiao Tung University, Hsin-Chu 300, Taiwan, ROC

^b Department of Electric Engineering, National Chiao Tung University, Hsin-Chu 300, Taiwan, ROC

^c Department of Applied Chemistry, National Chiao Tung University, Hsin-Chu 300, Taiwan, ROC

Received 11 October 2003; received in revised form 15 December 2003; accepted 17 December 2003

Abstract

An optical polymeric biochip system based on the complementary metal oxide semiconductor (CMOS) photo array sensor and polymeric enzyme biochip for rapidly quantitating uric acid in a one-step procedure was developed. The CMOS sensor was designed with N⁺/P-well structure and manufactured using a standard 0.5 μm CMOS process. The polymeric enzyme biochip was immobilized with uricase–peroxidase and used to fill the reacting medium with the sample. This study encompasses the cloning of the *Bacillus subtilis* uricase gene and expression in *Escherichia coli*, as well as the purification of uricase and measurement of its activity. The cloned uricase gene included an open reading frame of 1491 nucleotides that encodes a protein of approximately 55 kDa. The expression of the putative MBP-fusion protein involved approximately 98 kDa of the protein. The CMOS sensor response was stronger at a higher temperature range of 20–40 °C, with optimal pH at 8.5. The calibration curve of purified uric acid was linear in the concentration range from 2.5 to 12.5 mg/dL. The results obtained for serum uric acid correlated quite closely with those obtained using the Beckman Synchron method.

© 2004 Elsevier B.V. All rights reserved.

Keywords: CMOS photo array sensor; Polymeric enzyme biochip; Uricase; Peroxidase

1. Introduction

Uricase is an enzyme that participates in degrading purines by catalyzing the oxidative breakdown of uric acid to allantoin. This highly conserved enzyme is found in mammals (Keilin, 1959; Wallrath and Friedman, 1991), plants (Montalbini et al., 1997), fungi (Montalbini et al., 1999), yeasts (Yuichi et al., 2000; Yasuji et al., 1996; Adamek et al., 1990), and bacteria (Yamamoto et al., 1996). Uric acid, the primary end-product of purine metabolism, is present in biological fluids, such as blood and urine (Eswara et al., 1974). Various disease states increase the amount of uric acid in biological fluids. Such conditions cause gout, chronic renal disease, some organic acidemias, and Lesch–Nyhan syndrome (Burtic and Ashwood, 1994).

Several attempts have been made to fabricate uric acid sensors, using uricase (urate oxidase, EC 1.7.3.3.) as a bio-

catalyst (Yutaka et al., 1992; Bhargava et al., 1999; Nanjo and Guilbault, 1974; Uchiyama et al., 1991; Miland et al., 1996). Uricase catalyzes the in vivo oxidation of uric acid in the presence of oxygen to produce allantoin and CO₂ as oxidation products of uric acid, and hydrogen peroxide as a reduction product of O₂. Uricases from many microorganisms are used as diagnostic reagents for detection of uric acid. These enzymes exhibit high thermostability and are active over a wide pH range (Yuichi et al., 2000; Yasuji et al., 1996; Yamamoto et al., 1996; Schiavon et al., 2000). For example, the uricase of *Bacillus* sp. TB-90 demonstrated high activity and thermostability over a wide range of pH values.

Spectrophotometry at 293 nm is frequently used to detect the concentration of uric acid in solution. In Haeckel's method (Haeckel, 1976), the hydrogen peroxide produced by the uricase-catalyzed oxidation of uric acid is detected by the uricase-catalyzed oxidation of ethanol to acetaldehyde, coupled with the oxidation of the latter to acetate in the presence of NAD⁺ (or NADP⁺) and aldehyde dehydrogenase. The change in the absorbance of NADH (or NADPH) at 340 nm then is measured. An initial reading, to be used

* Corresponding author. Tel.: +886-3-5729-287;

fax: +886-3-5725-700.

E-mail address: tkwmll@mail.nctu.edu.tw (T.-K. Wu).

as a sample blank, must be taken. This method is a laborious and manual procedure. Furthermore, highly purified aldehyde dehydrogenase is not always readily available.

Various types of electrochemical enzyme sensors have been reported to be useful in uric acid determination. Nanjo and Guilbault (1974) developed an amperometric means of determining the quantity of uric acid in biological fluids. This method is based on the consumption of dissolved oxygen (Nanjo and Guilbault, 1974). Janchen et al. (1983) performed similar studies in the presence of oxygen. Such systems exploit the anodic electroactivity of peroxide. Unfortunately, its oxidation has been reported to require relatively high applied potentials (>0.4 V), and thus, is susceptible to interference from readily oxidizable molecules. Kulys and colleagues eliminated interference using horseradish peroxidase (HRP) to catalyze the reaction between H_2O_2 and hexacyanoferrate(II) and the reduction of the resulting hexacyanoferrate(III) at 0 V versus Ag/AgCl (Schiavon et al., 2000).

This paper describes the development of a polymeric enzyme biochip with a CMOS photosensor detection system to quantitate uric acid. In this study, a prototype CMOS array photosensor was designed and produced. To detect uric acid, a uricase–peroxidase-immobilized polymeric biochip was developed. The uricase gene of *Bacillus subtilis* was cloned, expressed in *Escherichia coli*, then the uricase was purified, and activity measured. Moreover, the polymeric biochip was immobilized simultaneously with uricase and peroxidase. Finally, we compare the measurements from 20 patients' serum uric acid samples using the CMOS biochip system to the Beckman Synchron analyzer.

2. Materials and methods

2.1. Optical detection system setup

Fig. 1 schematically depicts the optical arrangement of the enzyme biochip detection system built to detect serum uric acid using a polymeric enzyme biochip. To eliminate infrared light, a pure white light LED lamp (HB5-439AWCA, Russia) was used as the light source and the light intensity was controlled with an adjustable driver. The LED projects a light beam vertically through a mini-lens to generate a 1 mm diameter parallel light beam. The light beam passes through an interference filter wheel (a 520 nm interference filter, K43-069, Edmund, USA), then the self-developed polymeric biochip, and finally hits the surface of the prototypical CMOS photo array sensor. The polymeric biochip was immobilized with uricase–peroxidase and used to fill the reacting medium with the sample, the details of which are described below. The biochip is transparent so that the light could be transmitted to the sensor. The CMOS photo array sensor was designed with an N^+ /P-well structure and manufactured using a standard $0.5\ \mu\text{m}$ CMOS process. To transfer the current signal of the CMOS photo sensor lin-

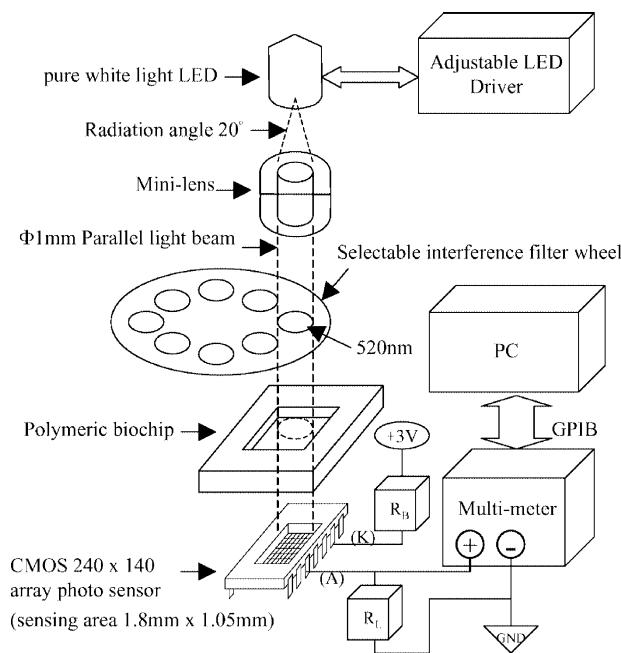


Fig. 1. Optical arrangement built with the CMOS photo array sensor and used for polymeric enzyme biochip detection (see the text for details).

early to the voltage signal, a bias resistor (R_b) was connected between a 3 V dc bias voltage source and the cathode (K) of the CMOS photosensor. A loading resistor (R_L) was connected between the anode (A) of the CMOS photo sensor and the ground of the bias voltage source. Then, the signal from the anode was used as the output voltage and connected to the positive probe of multi-meter (Agilent 34401A). The ground of the bias voltage source was connected to the negative probe of a multi-meter. The voltage signals were digitized and transferred as digital data to a personal computer with GPIB communication using a simple data collection program. The collected data were analyzed using Windows Excel that calculated the absorbance at 520 nm according to Beer–Lambert's law, i.e., $OD_{520\text{ nm}} = -\log(I/I_0)$, where I is final reaction light signal, I_0 is blank light signal. The results then were plotted graphically.

Fig. 2 shows a pixel structure and circuit diagram of the CMOS photo array sensor. Each pixel of the array sensor was implemented with a P–N junction diode using a P-well

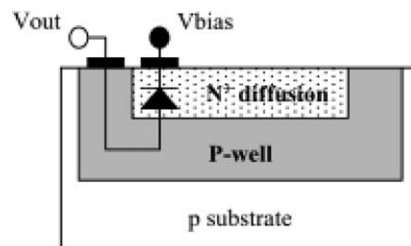


Fig. 2. The pixel structure of the CMOS photo array sensor. The P–N junction diode is implemented with N^+ diffusion and P-well and manufactured using a standard $0.5\ \mu\text{m}$ CMOS process.

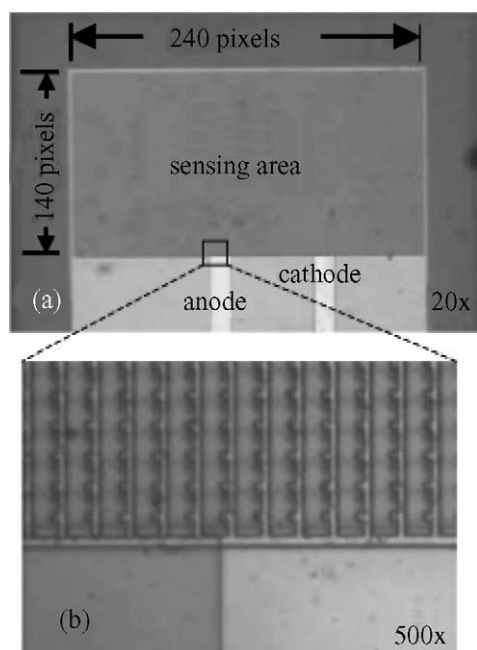


Fig. 3. (a) The layout of the 240×140 CMOS photo array sensor which occupies an area of $1.8 \text{ mm} \times 1.05 \text{ mm}$ and (b) the close-up microphotograph of the fabricated CMOS photo array sensor showing few pixels. Each pixel is $7.5 \mu\text{m} \times 7.5 \mu\text{m}$ in area.

and N^+ -active diffusion layer that could be fabricated using the $0.5 \mu\text{m}$ CMOS process. The array sensor was a 240×140 pixels in-parallel connection, as shown in Fig. 3a, with a single pixel size of $7.5 \mu\text{m} \times 7.5 \mu\text{m}$, as shown in Fig. 3b.

2.2. DNA manipulations

Cloning and transformation were performed essentially as described by Sambrook and Russell (2001). Genomic DNA from *B. subtilis* CCRC 14199 was obtained from the Culture Collection and Research Center (Food Industry Research and Development Institute, Hsin-Chu, Taiwan, ROC). *B. subtilis* uricase expression constructs were generated in a polymerase chain reaction (PCR). Briefly, the *B. subtilis* uricase gene was amplified using the plasmid DNA of *B. subtilis* (CCRC 14199) as a template, *rTth* DNA polymerase (Applied Biosystems) and the following primers: 5'-primer (5'-TCT AGA ATT CCA TAT GTT CAC AAT GGA TGA CCT G-3') and 3'-primer (5'-GCT GCA GAA GCT TCG CCG CTG GTT TGC CGC AGG-3'). The amplification reaction was performed in a total volume of $50 \mu\text{l}$: $0.5 \mu\text{l}$ template DNA; 10 pmol of each primer; 0.2 mM dNTPs (dATP, dGTP, dTTP, dCTP); 1.5 mM $\text{Mg}(\text{OAc})_2$; 1 U of *rTth* polymerase; and $3.3 \times \text{XL}$ *rTth* polymerase buffer. PCR amplification was conducted in a thermal cycler (GeneAmp PCR System 9700) with an initial denaturation for 1 min at 94°C , followed by 30 cycles (94°C , 15 s ; 58°C , 2 min ; 72°C , 8 min), and a final incubation for 10 min at 72°C . The amplified products were digested with *EcoRI* and *HindIII* and cloned into the *EcoRI/HindIII* pMAL (or pBluescript

II SK(+)), transformed into *E. coli* DH5 α competent cells and incubated at 37°C for 1 h with shaking. The culture was spread on LB plates containing ampicillin for antibiotic selection. X-gal and isopropylthio- β -D-galactoside (IPTG) were mixed and spread on LB plates for blue–white screening of recombinants.

2.3. Expression and purification of the fusion uricase

For protein expression, the pMAL-c2 system (BioLabs) was used to express the uricase gene. Cells that contain plasmids encoding fusion proteins under control of the lac promoter were grown to a concentration of $5 \times 10^8 \text{ cell/ml}$ at 37°C with shaking in a rich medium. IPTG was added to a final concentration of 0.3 mM , and the culture was grown for an additional 4 h . All subsequent steps were performed at 4°C or on ice. The cells were harvested by low-speed centrifugation, re-suspended in $1/10$ volumes of 10 mM Tris buffer pH 7.2 , and lysed by sonication. Cellular debris then was pelleted by high-speed centrifugation, and the supernatant was saved as a crude cellular extract.

The purification procedure was adopted from the pMAL-c2 protein fusion and purification system (Guan et al., 1988; Maina et al., 1988). The preparation of cross-linked amylose (BioLabs) and its use as an affinity chromatography matrix were as described by Kellerman and Ferenci (1982). Fusion proteins were purified from crude extracts by binding to cross-linked amylose in a column, and were eluted with 10 mM Tris buffer that contained 10 mM maltose (Guan et al., 1988; Maina et al., 1988).

2.4. Measurements of uricase activity

Uricase activity was routinely measured aerobically by the decrease in absorbance at 293 nm due to the enzymatic oxidation of uric acid (Yuichi et al., 2000; Yasuji et al., 1996; Yamamoto et al., 1996). The assay mixture contained 0.1 mM uric acid in 50 mM borate buffer (pH 8.5), and $10 \mu\text{l}$ of enzyme solution. One unit was defined as the amount of enzyme necessary to transform $1 \mu\text{mol}$ of uric acid into allantoin in 1 min at 25°C and pH 8.5 .

2.5. Preparation of the uricase–peroxidase conjugate

The protocol for preparing uricase–peroxidase was modified from Tresca et al. (1995). Briefly, 1 mg of peroxidase in 0.2 ml of 1 M phosphate buffer at pH 6.8 was made to react with 0.25 ml of freshly prepared 0.1 M sodium periodate for 20 min , and the peroxidase reagent was removed by dialysis against 1 mM sodium acetate buffer at pH 4.6 . Brown peroxidase-containing fractions were pooled and the uricase reagent was removed by dialysis against 0.1 M sodium carbonate buffer at pH 9.2 . Finally, the reaction medium was mixed with 0.2 ml of 4 mg/ml sodium borohydride and left for 2 h . It then was dialyzed against 10 mM phosphate buffer at pH 7.4 .

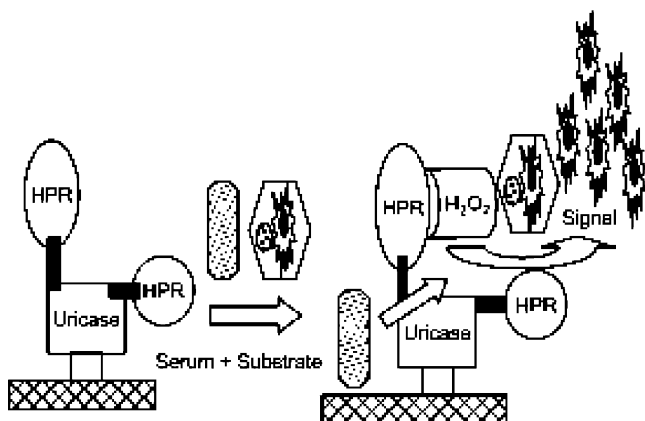


Fig. 4. Schematic polymeric enzyme biochip assay method for detecting uric acid using immobilized uricase and peroxidase. Serum uric acid is oxidized by uricase to produce allantoin and hydrogen peroxide. The hydrogen peroxide reacts with 4-aminoantipyrine and 3,5-dichloro-2-hydroxybenzene sulfonate in a reaction catalyzed by peroxidase to produce a colored product.

2.6. Immobilization of uricase–peroxidase conjugated on the biochip

An enzyme assay method using uricase–peroxidase probes was implemented, as shown in Fig. 4. Briefly, the sensing region of polymeric biochip was wetted with a solution of *p*-azidotetrafluorobenzaldehyde in methanol (25 mg/ml), air-dried in the dark, exposed to UV-light for 10 min, washed with methanol twice, then with distilled water and 0.01 M carbonate buffer at pH 9.5. For covalent fixation, a pre-activated biochip region was incubated in a solution of uricase–peroxidase in 0.01 M carbonate buffer at pH 9.5 for 30 min then was washed.

2.7. Measurement of serum uric acid with optical enzyme biochip system and Beckman Synchron analyzer

The absorbance of the biochip was detected with the optical enzyme biochip detection system. The system was especially adapted to quantitatively measure the absorbance of the biochip. A one part substrate solution (30 μ l) that contained 1 mM 4-aminoantipyrine, 4 mM 3,5-dichloro-2-hydroxybenzene sulfonate and 100 U/L ascorbate oxidase in 0.05 mM borate buffer at pH 8.5 and one part serum uric acid (30 μ l) was added to the biochip (immobilized with uricase–peroxidase). After reaction at room temperature for 1 min, the biochip was placed into the optical enzyme biochip detection system to measure the serum uric acid concentration. Hydrogen peroxide produced from the breakdown of uric acid (catalyzed by uricase) was measured by the oxidative coupling of 4-aminoantipyrine and 3,5-dichloro-2-hydroxybenzene sulfonate in the presence of peroxidase. To compare the detection ability of the developed biochip assay, a Beckman Synchron CX5

analyzer (USA) was used according to the manufacturer's instructions.

3. Results

3.1. Expression and purification of uricase

Genomic DNA from *B. subtilis* (CCRC 14199) was isolated, using a QIAamp tissue kit (Qiagen, Hilden, Germany). The uricase gene was amplified by PCR resulting in a fragment of 1491 bp. The 1491 bp *EcoRI/HindIII* DNA fragment was ligated into pMAL-c2 and pBluescript II SK(+), and the cloned plasmid was double-digested with *EcoRI* and *HindIII* (Fig. 5a). A uricase fusion protein was successfully purified from *E. coli* lysate only after it was enriched using an amylose column. The purified uricase fusion protein was eluted with maltose buffer and the fractions were pooled, concentrated, and analyzed by sodium dodecyl sulfate-polyacrylamide gel electrophoresis (Fig. 5b). For the uricase fusion protein, the major band on the gel had an apparent molecular mass of 98 kDa, corresponding to that predicted from the fusion gene sequence.

3.2. Measurements of uricase activity

The activity of the uricase expressed in *E. coli* and purified using SDS-PAGE was determined by a decrease in absorbance at 293 nm in the presence of uric acid. The effects of pH and thermal stability of the purified uricase also were examined. The pH stability was evaluated by incubation at different pH values (6–11) for 7 h. Optimal (100%) activity

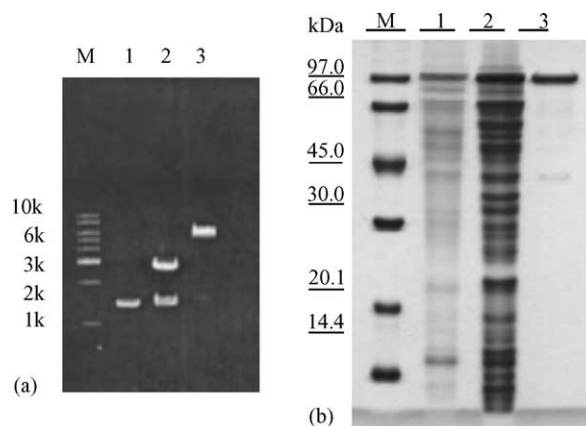


Fig. 5. (a) Agarose electrophoresis gel results of cloning. M, molecular markers; lane 1, the uricase gene (1491 bp DNA fragments) was amplified by PCR; lane 2, DNA fragments were ligated into pBluescript II SK(+), and digested by *EcoRI/HindIII*; lane 3, DNA fragment were ligated into pMAL, and were digested by *EcoRI/HindIII* and (b) SDS-PAGE analysis of the uricase fusion protein produced in *E. coli*, and purified on an amylose affinity spin column; lane 1, pellet; lane 2, crude extract; lane 3, eluate. The samples were loaded onto 12% polyacrylamide gels. The uricase fusion protein produced in *E. coli* had an apparent molecular mass of 98 kDa.

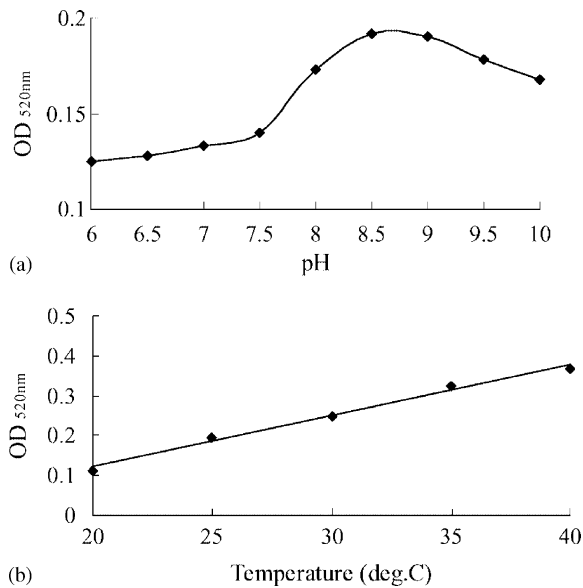


Fig. 6. Effect of pH and temperature on the absorbance of the uricase–peroxidase-immobilized biochip. (a) Effect of pH on the absorbance of the uricase–peroxidase-immobilized biochip and (b) effect of temperature on the absorbance of the uricase–peroxidase-immobilized biochip.

was found at pH values from 6 to 10. The thermal stability was examined by incubation for 30 min at different temperatures (4–80 °C) followed by cooling to room temperature. Complete inactivity was observed at 75 °C and 45% inactivity occurred at 70 °C. The residual activity maximum occurred between 4 and 55 °C.

3.3. Optimization of the uricase–peroxidase-immobilized biochip

The effects of temperature and pH on the uricase–peroxidase-immobilized biochip were evaluated. Fig. 6a plots the relationship between pH and the absorbance of the uricase–peroxidase-immobilized biochip in a single part substrate buffer (30 μ l) that contained 1 mM 4-aminoantipyrine, 4 mM 3,5-dichloro-2-hydroxybenzene sulfonate, 100 U/L ascorbic acid, and one part 5 mg/dL uric acid (30 μ l). The results showed that the absorbance of the uricase–peroxidase-immobilized biochip increased slowly with pH between 6 and 7.5, and then sharply increased with pH from 7.5 to 8.5; it finally declined as the pH increased from 8.5 to 10. The absorbance response was maximal at pH 8.5, which is the optimal pH for the uricase–peroxidase-immobilized biochip.

Fig. 6b plots the relationship between temperature and the maximum absorbance of the uricase–peroxidase-immobilized biochip. The reaction medium included one part substrate buffer (30 μ l) that contained 1 mM 4-aminoantipyrine, 4 mM 3,5-dichloro-2-hydroxybenzene sulfonate, 100 U/L ascorbic acid, and one part 5 mg/dL uric acid (30 μ l) in 0.05 mM borate buffer at pH 8.5. The result showed that the absorbance increased with the temperature from 20 to

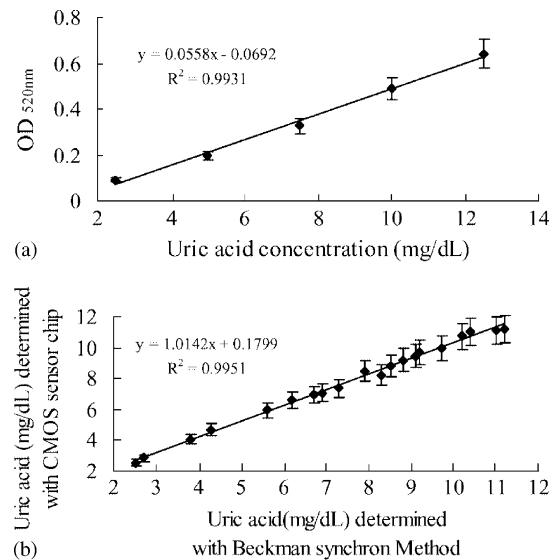


Fig. 7. (a) Calibration curve of purified uric acid concentration and absorbance at 520 nm using the uricase–peroxidase-immobilized biochip and (b) Comparison of serum uric acid results by Beckman Synchron method and polymeric enzyme biochip assay method.

40 °C and the absorbance–temperature curve had no peak. Hence, further experiments were performed at 25 °C, using 0.05 mM borate buffer at pH 8.5.

3.4. Evaluation of the uricase–peroxidase-immobilized biochip for measuring purified uric acid

In the application of the optical enzyme biochip detection system technology for assay of uric acid, success depends on combining of the efficiency of the immobilization enzyme reaction with that of photo-signal transduction. The calibration curve for purified uric acid was obtained using the uricase–peroxidase-immobilized biochip. Various quantities of uric acid (1, 2.5, 5, 7.5, 10, 12.5, 15 mg/dL) were added to a polymeric biochip that contained 4-aminoantipyrine, 3,5-dichloro-2-hydroxybenzene sulfonate and various concentrations of uric acid. From these measurements, a calibration curve was obtained to evaluate of uric acid screening using the CMOS photosensor technology. Fig. 7a plots the dose response curve between the purified uric acid concentration and the absorbance of the uricase–peroxidase-immobilized biochip. A calibrated value above or equal to a blank plus three standard deviations was considered positive. As shown by the calibration curve, the response was linear between 2 and 12.5 mg/dL. The regression line for purified uric acid was $y = 0.0558x - 0.0692$ and the correlation coefficient had a value of $r^2 = 0.9931$.

3.5. Application of the optical polymeric biochip detection system for measuring serum uric acid

Serum samples from apparently healthy adults and patients with gout, leukemia, toxemia of pregnancy, and

nephrolithiasis were collected from the Executive Yuan, Department of Health Hsin Chu Hospital. Serum samples were diluted 1:1 in substrate solution, then placed directly on the optical enzyme biochip detection system, and the concentration of uric acid present was estimated from a calibration plot. Results were within the linear range of the reaction, and the calibration graph was from 2.5 to 12.5 mg/dL for serum uric acid. The results obtained by the optical enzyme biochip system were compared with those obtained using the Beckman Synchron analyzer. As shown in Fig. 7b, the results indicated that the measured serum uric acid for 20 different serum sample using the optical enzyme biochip detection system correlated closely to results using the Beckman Synchron analyzer. The regression line for serum uric acid was $y = 1.0142x + 0.1799$ and the correlation coefficient was $r^2 = 0.9951$. Results for serum uric acid obtained using a biochip did not significantly differ from those obtained using a Beckman Synchron analyzer.

4. Discussion

This study used a CMOS photosensor, a biochip containing enzyme probes, in a rapid and sensitive method for accurately quantitating and directly monitoring enzyme-catalyzed reactions. The CMOS process is well established in the microelectronic industry, and has the potential to produce low-cost photosensors designed with an N⁺/P-well structure. By integrating an LED, a polymeric biochip, and a biased CMOS photosensor with a digitizing device, a low-cost optical detection system could be built. Traditionally, glass has excellent properties for mechanics, thermodynamics and optics, and is popular as a biochemical material. The disadvantage of using glass is difficulties in processing and forming. However, polymer materials are superior in price, easy formation and easy mass production. Detection of uric acid using a biochip system is important to the clinical field of biotechnology, and depends on the simultaneous immobilization of uricase and peroxidase on the biochip. Two factors determine the overall response of the biochip in such a system: the influence of temperature and pH on enzyme activity, and the effect of temperature and pH on the generated absorbance. Temperature is an essential factor in enzymatic reactions. The effect of temperature on the biochip response was investigated over the range between 20 and 40 °C. The results indicate that the response of the CMOS sensor is stronger at higher temperatures in the tested temperature range of 20–40 °C. The optimal pH for immobilizing uricase and peroxidase on the biochip is 8.5. The calibration curve was accurate from 2.5 to 12.5 mg/dL for purified uric acid. Measuring the concentration of serum uric acid in human serum samples demonstrates the usefulness of the assay in clinical chemistry. The results obtained agreed reasonably with those obtained by the Beckman Synchron method. Uric acid is oxidized by uricase to produce allantoin and hydrogen peroxide.

The hydrogen peroxide reacts with 4-aminoantipyrine and 3,5-dichloro-2-hydroxybenzene sulfonate, in a reaction catalyzed by peroxidase to produce a colored product. The Beckman Synchron system reagent was used to measure the uric acid concentration by a timed-end-point method (Fossati et al., 1980). This system automatically apportions the appropriate sample and reagent volumes into a cuvette and monitors the change in absorbance at 520 nm where the change in absorbance is directly proportional to the concentration of uric acid in the sample.

The development of the optical enzyme biochip detection system, a device that includes a bioreceptor (for example, an enzyme) and a signal transducer (COMS photosensor) is presented here. When the analyte interacts with the bioreceptor, the resulting complex produces a change, which is translated into a measurable efferent (such as an electrical signal) by the transducer. The first application of the optical enzyme biochip detection system was in an enzyme-based biochip developed to detect uric acid. The application detects uric acid by the immobilization of the enzyme uricase–peroxidase as a bioreceptor. In the optical enzyme biochip detection system, the measured enzyme-catalyzed reactions and produced hydrogen peroxide directly with the quantity of uric acid. The catalysis by the enzymes and the small size of the CMOS photosensor, allow the continuous monitoring of the release of hydrogen peroxide from uric acid. Accordingly, data is presented demonstrating that the optical enzyme biochip detection system is useful for the detection of uric acid in human clinical samples.

The IC system designed for the microchip photosensor elements and associated data treatment is based on complementary metal oxide semiconductor (CMOS) technology. The development and evaluation of various elements of the DNA biosensor microchip technology have been described. The design of the gene probe immobilization techniques on the biosensor substrates as well as the development of integrated electro-optic systems on the IC biochip using a phototransistor multi-array system previously have been discussed. For example, the quantitation of HIV-1 using sequence-specific fluorescent-labeled DNA probes and hybridization on the nitrocellulose sampling platform system was described (Vo-Dinh et al., 1999). In another example, Stokes et al. (2001) evaluated the combined effectiveness of the IC biochip and antibody probe-based assay and determined that it yielded exceptional quantitative ability, sensitivity, and selectivity (Stokes et al., 2001). In this system, the sampling platform is a cellulose membrane that is exposed to *E. coli* and subsequently analyzed using a sandwich immunoassay involving a Cy5-labeled antibody probe.

A focus of our laboratory is the development of optical enzyme biochip assay technology and quantitation of various enzymes using CMOS technology. These studies include the design of the enzyme probe immobilization techniques on the polymeric biochip as well as the development of a photosensor using CMOS technology. We describe an application that detects uric acid by immobilized uricase–peroxidase

probes. Measurements of enzyme-catalyzed reactions allow for direct monitoring of the degradation of the uric acid in a quantitative manner. In conclusion, the use of a photosensor based on CMOS technology will lead to the development of low-cost diagnostic biochips for medical applications.

Acknowledgements

This work was supported by National Chiao Tung University of Taiwan (Republic of China). The authors would like to thank Dr. Tin-Yin Liu, Director of the Food Industry Research and Development Institute, Dr. Tsung-Chain Chang, Professor of National Cheng-Kung University, Dr. Bill Franke, Professor of Nantai Technology University, for valuable discussions.

References

- Adamek, V., Suchova, M., Demnerova, K., Kralova, B., Fort, I., Morava, P., 1990. Fermentation of *candida utilis* for uricase production. *J. Ind. Microbiol.* 6, 85–90.
- Bhargava, A.K., Lal, H., Pundir, C.S., 1999. Discrete analysis of serum uric acid with immobilized uricase and peroxidase. *J. Biochem. Biophys. Methods* 39, 125–136.
- Burtic, C.A., Ashwood, E.R., 1994. Teitz Textbook of Clinical Chemistry, second ed. WB Saunders, Philadelphia.
- Eswara, U.S., Dutt, H., Mottola, A., 1974. Determination of uric acid at the microgram level by a kinetic procedure based on a pseudo-induction period. *Anal. Chem.* 46, 1777.
- Fossati, P., Prencipe, L., Berti, G., 1980. Use of 3,5-dichloro-2-hydroxybenzenesulfonic acid/4-aminophenazone chromogenic system in direct enzymic assay of uric acid in serum and urine. *Clin. Chem.* 26, 227–231.
- Guan, C., Li, P., Riggs, P.D., Inouye, H., 1988. Vectors that facilitate the expression and purification of foreign peptides in *E. coli* by fusion to maltose-binding protein. *Gene* 67, 21–30.
- Haackel, R., 1976. The use of aldehyde dehydrogenase to determine H₂O₂-producing reactions. I. The determination of the uric acid concentration. *J. Clin. Chem. Clin. Biochem.* 14, 101–106.
- Janchen, M., Walzel, G., Neef, B., Wolf, B., Scheller, F., Kuhn, M., 1983. Uric acid determination in dilute serum with an enzyme electrochemical and enzyme-free sensor. *Biomed. Biochim. Acta* 9, 1055–1059.
- Keilin, J., 1959. The biological significance of uric acid and guanine excretion. *Biol. Rev.* 34, 265–296.
- Kellerman, O.K., Ferenci, Y., 1982. Maltose-binding protein from *Escherichia coli*. *Methods Enzymol.* 90, 459–467.
- Maina, C.V., Riggs, P.D., Granda, A.G., Slatko, B.E., Moran, L.S., Tagliamonte, J.A., 1988. An *E. coli* vector to express and purify foreign proteins by fusion to and separation from maltose-binding protein. *Gene* 74, 365–373.
- Miland, E., Ordieres, A.J.M., Blanco, P.T., Smyth, C.O., 1996. Poly(*o*-aminophenol)-modified bienzyme carbon paste electrode for the detection of uric acid. *Talanta* 43, 785–796.
- Montalbini, P., Redondo, J., Caballero, J.L., Cardenas, J., Pineda, M., 1997. Uricase from leaves: its purification and characterization from three different higher plants. *Planta* 202, 277–283.
- Montalbini, P., Aguilar, M., Pineda, M., 1999. Isolation and characterization of uricase from bean leaves and its comparison with uredospore enzyme. *Plant Sci.* 147, 139–147.
- Nanjo, M., Guilbault, G.G., 1974. Enzyme electrode sensing oxygen for uric acid in serum and urine. *Anal. Chem.* 46, 1769–1772.
- Sambrook, J., Russell, D.W., 2001. Molecular Cloning: A Laboratory Manual. Cold Spring Harbor Laboratory Press, Cold Spring Harbor, NY.
- Schiavon, O., Calicati, P., Ferruti, P., Veronese, F.M., 2000. Therapeutic proteins: a comparison of chemical and biological properties of uricase conjugated to linear or branched poly(ethylene glycol) and poly(*N*-acryloylmorpholine). *Il Farmaco* 55, 264–269.
- Stokes, D.L., Griffin, G.D., Vo-Dinh, T., 2001. Detection of *E. coli* using a microfluidics-based antibody biochip detection system. *Fresenius J. Anal. Chem.* 369, 295–301.
- Tresca, J.P., Ricoux, R., Pontet, M., Engler, R., 1995. Comparative activity of peroxidase-antibody conjugates with periodate and glutaraldehyde coupling according to an enzyme immunoassay. *Ann. Biol. Clin.* 53, 227–231.
- Uchiyama, S., Shimizu, H., Hasebe, Y., 1991. Chemical amplification of uric acid sensor responses by dithiothreitol. *Anal. Chem.* 66, 1873–1876.
- Vo-Dinh, T., Alarie, J.P., Isola, N., Landis, D., Wintenberg, A.L., Ericson, M.N., 1999. DNA biochip using a phototransistor integrated circuit. *Anal. Chem.* 71, 358–363.
- Wallrath, L.L., Friedman, T.B., 1991. Species differences in the temporal pattern of drosophila urate oxidase gene expression are attributed to trans-acting regulatory changes. *Proc. Natl. Acad. Sci. U.S.A.* 88, 5489–5493.
- Yuichi, H., Tetsuhiko, S., Hajime, I., 2000. Cloning, sequence analysis and expression in *Escherichia coli* of the gene encoding a uricase from the yeast-like symbiont of the brown planthopper, *Nilaparvata lugens*. *Insect Biochem. Mol. Biol.* 30, 173–182.
- Yamamoto, K., Kojima, Y., Kikuchi, T., Shigyo, T., Sugihara, K., Takashio, M., 1996. Nucleotide sequence of the uricase gene from *Bacillus* sp. TB-90. *J. Biochem.* 119, 80–84.
- Yasuji, K., Toshio, I., Erichi, N., 1996. Cloning, sequence analysis and expression in *Escherichia coli* of the gene encoding the *candida utilis* urate oxidase. *J. Biochem.* 120, 969–973.
- Yutaka, A., Hiroshi, I., Hiroomi, N., Tsugutoshi, A., Mitsutak, Y., 1992. Effects of serum bilirubin on determination of uric acid by the uricase-peroxidase coupled reaction. *Clin. Chem.* 38, 1350–1352.